Equilibrium and Kinetic Parameters of the Sequence-Specific Interaction of *Escherichia coli* RNA Polymerase with Nontemplate Strand Oligodeoxyribonucleotides†

Andrew M. Fedoriw, Huaying Liu, Vernon E. Anderson, and Pieter L. deHaseth*

Department of Biochemistry, Case Western Reserve University, Cleveland, Ohio 44106-4935

Received April 29, 1998; Revised Manuscript Received June 24, 1998

ABSTRACT: The specific recognition by *Escherichia coli* RNA polymerase of single-stranded oligodeoxyribonucleotides (oligos) with the sequence of the −10 promoter region on the nontemplate strand has been studied. Binding was monitored by observing the increase in fluorescence of 2-aminopurine residues incorporated in the oligos. The effects of salt on the rates of formation and dissociation of RNA polymerase·oligo complexes are relatively small, from which we conclude that electrostatic interactions contribute minimally to the favorable binding free energy. From the convex temperature dependence of ln K_a (K_a is the equilibrium association constant), we infer that a large apparent negative heat capacity, of 1−2 kcal M^{-1} K^{-1}, accompanies complex formation, which is interpreted as due to a conformational change in RNA polymerase. Contrary to expectation, the forward rate constant for binding of oligos is more than 10-fold smaller than that for open complex formation at strong promoters. This suggests that in comparison to an oligo, promoter DNA may be better able to accelerate this required conformational change in the RNA polymerase. Oligo binding was shown to compete with the interaction between RNA polymerase and promoters, indicating that the two bind to overlapping sites on the RNA polymerase

Promoter recognition by *Escherichia coli* RNA polymerase (RNAP)[1] depends primarily on two regions of DNA sequence conservation, located about 10 and 35 base pairs upstream of the start site. Recognition of these −10 and −35 promoter elements is carried out by regions 2.4 and 4.2, respectively, of the major sigma factor, σ^{70}, of *Escherichia coli* (*1*). In a functional complex between RNAP and a promoter, the base pairing of the promoter DNA has been found to be disrupted over a stretch of 12−15 base pairs, including the start site of transcription (*2*). Neither the disruption of the base pairing nor the maintenance of the strand-separated "open" complex requires an external source of energy. Several studies have indicated that aromatic amino acid residues of conserved region 2.3 of σ^{70} may be involved in the RNAP-induced strand separation process (*3*−*7*), likely by directly binding the nontemplate strand of promoter DNA in the region where the strand separation occurs.

At least three lines of evidence indicate that RNAP primarily interacts with the nontemplate strand of the promoter in the −10 region and downstream: First, the classic chemical probing studies by Gilbert and co-workers (*2*) show that most of the effects of bound RNAP on the reactivity of promoter DNA with various chemical probes are on the nontemplate strand. Second, it has been shown that sequence-specific recognition of the −10 promoter element involves the identity of bases of the nontemplate strand (*8*). Third, RNAP holoenzyme interacts in a sequence-specific fashion with single-stranded nontemplate DNA, but not with the template DNA (*7*, *9*−*14*).

Formation of the open RNAP−promoter complex is a multistep process, involving conformational changes not only in the DNA (strand separation) but also in the RNAP (*15*, *16*). Despite the complexity of the process, substantial progress has been made in the characterization of the various intermediates involved. Thus, it now appears that the conformational change in the RNAP is the rate-limiting step on this reaction pathway (Tsodikov and Record, personal communication). To gain a better understanding of the interaction of RNAP with single-stranded DNA in the region of strand separation, we have characterized this interaction directly, building upon recent studies that demonstrated the specificity of this interaction. We describe here our experiments on the sequence-specific recognition of single-stranded oligodeoxyribonucleotides (oligos). We also determined the salt and temperature dependence of the interaction. We interpret the results to indicate that just as is the case for the interaction of RNAP with promoters, RNAP has to undergo a conformational change in order to interact with the oligos. Contrary to expectation, the forward rate constant for binding of the oligos is more than 10-fold smaller than that for open complex formation at strong promoters, which suggests that promoter DNA, but not an oligo, may be able to accelerate a required conformational change in the RNAP.

† This work was supported by Grants GM 31808 (P.L.H.) and GM 36562 (V.E.A.) from the National Institutes of Health. The core facility at Case Western Reserve University (oligodeoxyribonucleotide synthesis) is supported by USPHS Grant P30CA43703.

* Address correspondence to this author at the Department of Biochemistry, School of Medicine, Case Western Reserve University, 10900 Euclid Ave., Cleveland OH 44106-4935. Telephone: 216 368 3684. Fax: 216 368 4544.

[1] Abbreviations: oligo, oligodeoxyribonucleotide; ss DNA, single-stranded DNA; RNAP, RNA polymerase; 2-AP, 2-aminopurine.

S0006-2960(98)00980-5 CCC: $15.00 © 1998 American Chemical Society
Published on Web 07/29/1998

MATERIALS AND METHODS

Materials. *E. coli* RNAP holoenzyme prepared by the method of Burgess and Jendrisak (*17*) was further purified by chromatography on phosphocellulose in the presence of 50% glycerol, as described (*18*). The concentrations of RNAP reported here are those of the active holoenzyme; our preparations were 50 ± 10% active as determined by titration of a known amount of promoter DNA with purified RNAP and monitoring open complex formation using a gel shift assay. Because of our finding that oligo and promoter DNA occupy functionally overlapping sites on RNAP (see Figure 7), activities determined in this fashion should be relevant to our studies on the interaction of RNAP with oligos. Oligos containing 2-AP substitutions were purchased from core facilities at Case Western Reserve University and at the University of Wisconsin, Madison. Concentrations were determined spectroscopically, using the following molar extinction coefficients (in OD_{260}/M) for the bases in single-stranded DNA: dA, 15300; dC, 7400; dG, 11800; dT, 9300; and d(2-AP), 1000. The molar extinction coefficient of an oligo was calculated from the contributions of its constituent bases. Unmodified oligos were from Gibco-BRL and the Case Western Reserve University core facility. Heparin was from Sigma.

Oligo Competition Experiments. Ten microliters of RNAP (100 nM) and oligos at various concentrations were incubated for 15 min at 37 °C in transcription buffer [30 mM HEPES (pH 7.6), 100 mM KCl, 10 mM $MgCl_2$, 0.1 mM DTT]. Ten microliters of radiolabeled promoter DNA (4 nM; 40 000 cpm), with consensus −10 and −35 regions [e.g., see (*16*)], was added, and incubation was continued for 10 min. After addition of heparin to 50 μg/mL, the reactions were loaded onto prerunning 4% nondenaturing polyacrylamide gels in 0.04 M Tris−acetate, 0.001 M EDTA to separate free from RNAP-bound promoter DNA. Binding was quantified by phosphor imaging (Molecular Dynamics).

Stopped-Flow Experiments. Binding reactions were carried out in transcription buffer (see above), containing10% glycerol, on an Applied Photophysics SX18MV stopped-flow spectrophotometer in the fluorescence mode as described (*19*). The excitation monochromator was set at 315 nm, and a 350 nm "cut on" filter (transparent to light with a wavelength greater than 350 nm) was used for the emitted light. Excitation monochromator slits were set at 2 nm. Glycerol was a necessary component of all mixes as the RNAP is stored in 50% glycerol; both the ssDNA and the RNAP solutions loaded in the syringes of the instrument were adjusted to contain the same concentration (10%) of glycerol in order to get optimal mixing. Typically, the final concentration of active RNAP was 15 nM.

Data Analysis. Initial data analysis was carried out using software provided by Applied Photophysics. The experiments were conducted with the oligos in at least 4-fold molar excess over the RNAP so that the kinetics would be pseudo first order. The data were fit to the equation:

$$y = \mathrm{Amp}[1 - \exp(-k_{obs}t)] + F_0 \qquad (1)$$

where y is the fluorescence signal at wavelengths greater than 350 nm, t is the time in seconds after mixing DNA and RNAP, k_{obs} is the pseudo-first-order rate constant, Amp is the observed amplitude, and F_0 is the observed fluorescence at time zero. Each reported value of k_{obs} is the average of data collected in five or more separate mixing events. Under any set of conditions, k_{obs} was obtained at several oligo concentrations. Initial data analysis was by modeling the interaction as a simple one-step reaction. The parameters k_a and k_d (corresponding to the rate constants for the forward and reverse reactions as represented by eq 4, below) were obtained from the slope and intercept of a linear fit of the data to the equation:

Oligo Sequences

Consensus Sequence Used:	
	5'-CGG *AA*C TAT AAT TGA CTC ATA CGG
Mutant Sequences:	
T-12A	5'-CGG *AA*C AAT AAT TGA CTC ATA CGG
A-11C	5'-CGG *AA*C TCT AAT TGA CTC ATA CGG
T-10G	5'-CGG *AA*C TAG AAT TGA CTC ATA CGG
A-9T	5'-CGG *AA*C TAT TAT TGA CTC ATA CGG
A-8G	5'-CGG *AA*C TAT AGT TGA CTC ATA CGG
T-7C	5'-CGG *AA*C TAT AAC TGA CTC ATA CGG
Blank	5'-CGG *AA*C ACG TGC TGA CTC ATA CGG

NOTE: *A* = 2-aminopurine

FIGURE 1: Sequences of the oligos used in this work. ***A*** denotes 2-AP.

$$k_{obs} = k_a[\mathrm{oligo}] + k_d \qquad (2)$$

Reported errors in individual values of k_a and k_d are standard errors, as determined in fitting the data. Whenever multiple determinations had been obtained, averages of the values and standard deviations have been reported.

To obtain equilibrium binding constants from the data, the amplitudes (Amp in eq 1) of the exponential fits were averaged for each [oligo], and fit to a rectangular hyperbola:

$$\mathrm{Amp} = \frac{F_{max}[\mathrm{oligo}]}{[\mathrm{oligo}] + K_d} \qquad (3)$$

Here K_d is the observed dissociation constant and F_{max} the limiting value of the amplitude at infinite [oligo]; the reciprocal value of K_d will be referred to as K_a, the equilibrium association constant. Other data manipulations were carried out as described in the text.

RESULTS

The synthetic oligos used in this work are shown in Figure 1. The sequence of the consensus oligo was designed to minimize secondary structure; the other oligos shown differ from each other in the incorporation of nonconsensus bases throughout the −10 region. All bear two 2-AP bases at positions −14 and −15 in a numbering scheme where the most downstream T of the −10 region is −7, reflecting its position with respect to the start site of most promoters. We had previously observed an increase in 2-AP fluorescence upon addition of RNAP to promoters bearing 2-AP substitutions between positions −7 and +3 (*19*). The fluorescence not only of the 2-AP-substituted oligos described above but also of oligos containing downstream 2-AP substitutions at positions +1 and +3 (data not shown) was similarly observed to increase upon addition of RNAP, providing a spectroscopic

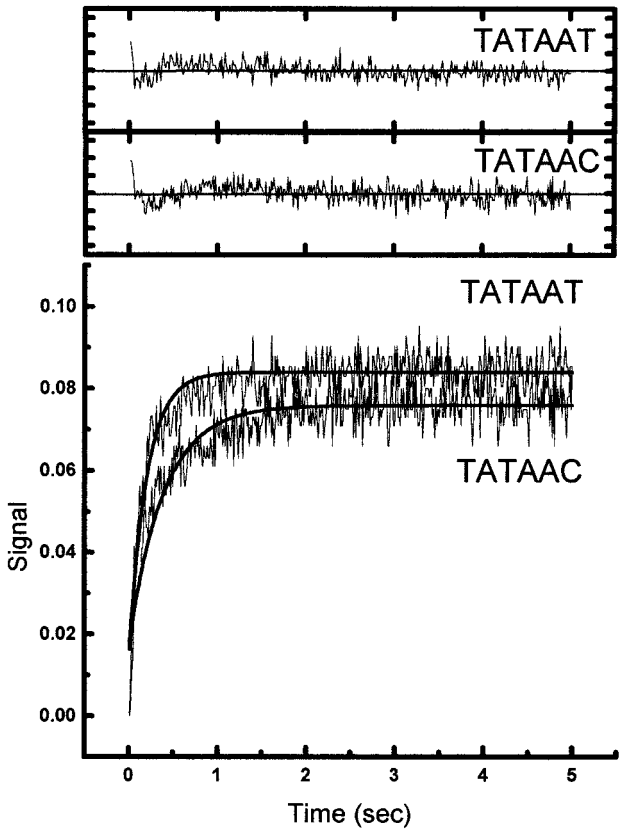

FIGURE 2: Time dependence of the increase in fluorescence upon mixing RNAP with the consensus and the T-7C oligos. Final concentrations were: [RNAP], 15 nM; [oligo], 400 nM; the temperature was 25 °C. See Materials and Methods for additional experimental details. The traces shown are averages of at least 5 individual mixing events, and commence at the origin. The smooth lines shown are for single-exponential fits with $k_{obs} = 5.0 \pm 0.2$ and 2.6 ± 0.1 s^{-1}, for the consensus and T-7C oligos, respectively. Differences between the fitted and measured values (residuals) are shown in the top part of the figure.

assay for their interaction. However, oligos containing 2-AP at positions −9 and −8 (in the −10 element) or at positions −5 and −4 (just downstream of −10) did not generate a measurable signal upon addition of RNAP (data not shown). Using oligos containing 2-AP substitutions at +1 and +3, we had previously verified that the presence of A's at −15 and −14, rather than the "TG" sequence conserved in some promoters (*20*), did not affect the observed rates (data not shown). For the studies reported here, we chose 2-AP substitutions at −15 and −14 (as shown in Figure 1), rather than at +1 and +3, as the former are closer to the −10 sequence. The presence of two, rather than one, 2-AP substitutions provided a useful increase in the measured fluorescence signal. In comparisons between oligos with the 2-AP upstream or downstream of the −10 sequence, similar results were obtained, with few exceptions (noted below).

To study the kinetics of the interaction between RNAP and oligos, solutions of RNAP and 2-AP substituted oligos were mixed in a stopped-flow spectrophotometer, and the observed increase in 2-AP fluorescence was monitored over a time interval of 5 s, sufficient for adequate definition of the end point of the reaction. Representative traces are shown in Figure 2, from which the values of k_{obs} for [oligo] = 400 nM, plotted in Figure 3, were determined. As can be seen, single exponentials (eq 1), with $k_{obs} = 5.0 \pm 0.2$ s^{-1} and Amp = 0.072 ± 0.002 for the consensus oligo, and with $k_{obs} = 2.6 \pm 0.1$ s^{-1}, and Amp = 0.060 ± 0.002 for the T-7C oligo, fit the data quite well. However, a fast phase is also evident between 0 and 0.1 s, where eq 1 represents a less satisfactory description of the time dependence as evidenced by the residuals shown at the top of the figure. A double-exponential function (eq 1a) was also used to analyze the data:

$$y = \text{Amp1}[1 - \exp(-k_{obs1}t)] + \text{Amp2}[1 - \exp(-k_{obs2}t)] + F_o \quad (1a)$$

The fast phase is characterized by k_{obs1};Amp1 with values of 13 ± 1 s^{-1};0.074 ± 0.004 and 11 ± 2 s^{-1};0.056 ± 0.004, respectively, for the consensus and T-7C oligos, and the slow phase by k_{obs2};Amp2 with values of 1.4 ± 0.2 s^{-1};0.022 ±

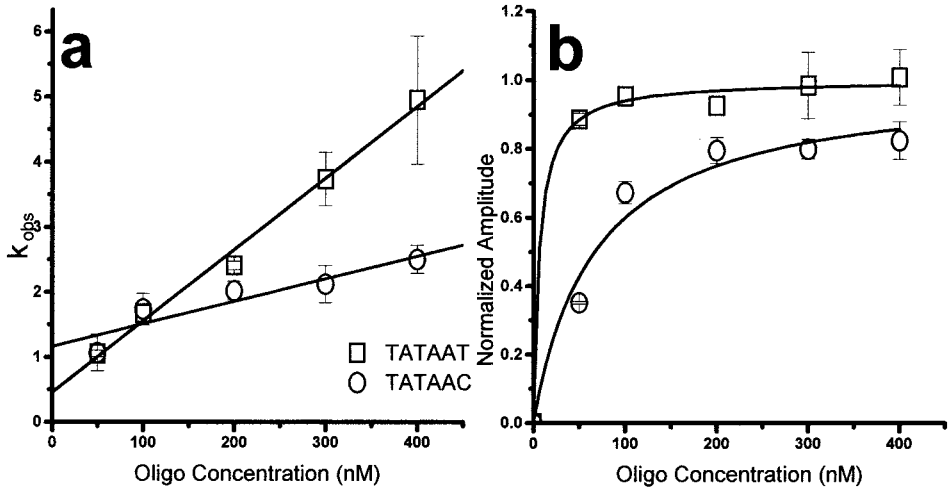

FIGURE 3: Representative data for two of the oligos used. All determinations carried out at 25 °C. (a) Plots of k_{obs} (each data point represents an average of at least 5 individual traces) as a function of [oligo] for the consensus and the T-7C oligos. The slopes of the lines yield k_a [$(1.1 \pm 0.1) \times 10^7$ M^{-1} s^{-1} and $(3.4 \pm 0.1) \times 10^6$ M^{-1} s^{-1} for the consensus and T-7C oligos, respectively]; k_d was determined from the intercepts (0.5 ± 0.1 s^{-1} and 1.2 ± 0.2 s^{-1} for the consensus and T-7C oligos, respectively). (b) Plots of the amplitudes of the fluorescence increase observed at each [oligo] (averages of at least 5 traces) versus [oligo]. From these saturation curves, the equilibrium binding constants can be determined ($K_d \leq 7 \pm 2$ nM for the consensus and $K_d = 70 \pm 20$ nM for the T-7C oligo). See Table 1 for average values from several experiments for k_a, k_d, and $K_a = 1/K_d$.

Table 1: Sequence Dependence of RNAP−Oligo Interaction

	equilibrium		kinetics	
oligo	K_a (M^{-1})[a]	k_a/k_d (M^{-1})	k_a (M^{-1} s^{-1})[b]	k_d (s^{-1})[b]
−10 TATAAT	$(5 \pm 3) \times 10^7$ [c]	$(2 \pm 1) \times 10^7$	$(7 \pm 2) \times 10^6$ [c]	0.4 ± 0.2[c]
−10 TATAAC	$(1.6 \pm 0.2) \times 10^7$ [d]	$(7 \pm 3) \times 10^6$	$(5 \pm 1) \times 10^6$ [d]	0.7 ± 0.2[d]
−10 ACGTGC	$(8 \pm 2) \times 10^6$	$(8.4 \pm 0.2) \times 10^5$	$(1.1 \pm 0.2) \times 10^6$	1.3 ± 0.05

[a] Determined from the amplitudes of the observed fluorescence signal (eq 3). [b] Determined from plots of k_{obs} versus [oligo]. [c] Average (±SD) of 6 separate determinations, each based on 5 or more individual mixing events on the stopped-flow spectrophotometer. [d] Average (±SD) of 3 separate determinations, each based on 5 or more individual mixing events on the stopped-flow spectrophotometer.

0.003 and 1.2 ± 0.1 s^{-1};0.030 ± 0.003, respectively, for the consensus and T-7C oligos. Equation 1a provides a clearly improved fit in the 0−0.1 s range, but overall the difference between the single- and double-exponential fits is less than the noise in the data. We also noticed that the values for both the amplitude and the k_{obs} obtained with eq 1a varied considerably and unpredictably as a function of oligo concentration, or in the comparison of duplicate experiments. To better define the fast phase, we have carried out experiments where all the data collection was in the 0−0.5 s interval (data not shown). Over this time interval, the rate constant as determined by eq 1 was independent of oligo concentration for the range 50−400 nM, where significant variation is seen for k_{obs} of the slow phase (see Figure 3). This behavior is unexpected for the formation of a collision complex. It is currently unclear what process gives rise to the fast phase, or even whether this phase is relevant to the interaction between RNAP and oligo. From here on, we focus exclusively on the slower phase of the reaction; all values for k_{obs} reported are from single-exponential fits to the data.

Representative data for the dependence of k_{obs} on [oligo] are shown in Figure 3a for the consensus and T-7C oligos (see Figure 1). Each data point represents the average of at least five traces. The data were interpreted in terms of a simple one-step reaction, as shown in eq 4, below:

$$\text{RNAP} + \text{oligo} \underset{k_d}{\overset{k_a}{\rightleftharpoons}} \text{RNAP}\cdot\text{oligo} \qquad (4)$$

k_a was obtained as the slope of the plots shown in Figure 3a, and k_d values were obtained from the intercept with the *y*-axis. Values for k_d may also be obtained directly, by preforming an RNAP−oligo complex, and then challenging it with either heparin or a large excess of oligo lacking 2-AP substitutions, to capture the free RNAP and pull the equilibrium in the direction of the dissociation of the 2-AP-substituted oligo from its complex with RNAP. In experiments using oligos with the 2-AP substitutions at positions +1 and +3, similar k_d values were obtained with the use of either heparin or oligo scavengers; these values were also similar to those determined from the intercepts of plots such as those shown in Figure 3a.

Equilibrium binding constants can be calculated from the ratio of the rate constants k_a and k_d as well as from the titration of the amplitude of the total change in fluorescence intensity observed at different oligo concentrations (eq 3), as shown in Figure 3b. Note that for the consensus oligo in this experiment only an upper limit of K_d could be established. The averages of values obtained in several experiments such as those shown in Figure 3a,b have been collected in Table 1. The T-7C substitution is seen to cause a 2-fold increase in k_d and a smaller reduction in k_a. The net effect of this substitution is a 3-fold decrease in the value of the equilibrium binding constant, regardless of whether K_a ($=1/K_d$) values determined from the amplitudes are compared, or ratios of k_a/k_d, although the values of the former are about 2.5-fold greater (see below).

The results of a systematic study of substitutions at positions in and next to the −10 region on K_d, k_d/k_a, k_a, and k_d are shown in Figure 4. At each position, we chose a base which, when substituted in promoters, would most dramatically reduce promoter strength [e.g., see (*21*)]. In agreement with previous studies (*7*, *9*−*14*), it is seen that the interaction is sequence-specific, although not at all positions tested. The effects of substitutions at −7 and −8 are evident in all four panels of Figure 4, while the substitution at −9 appears to not affect k_a. Substitutions at positions −10 to −12 were not found to significantly affect the kinetics or the equilibrium of the interaction. Note that an oligo bearing substitutions at each of the six positions of the −10 region ("ACGTGC") has substantially lower k_a and higher k_d values, as well as reduced K_a, compared to oligos with T-7C or A-8G substitutions. Similar patterns have been observed for an analogous series of oligos containing 2-AP at positions +1 and +3, with one exception. The T-12A substitution does not appear to affect oligos with the 2-AP at −14 and −15 (see Figure 4), but the same substitution in oligos with the 2-AP at +1 and +3 leads to a 75% reduction in k_a and a 2-fold increase in k_d as compared to the values of the consensus oligo (data not shown). The latter result is more akin to that obtained in competition assays (*13*), where a T-12C substitution was found to reduce the affinity by approximately 20-fold. Even so, it is interesting that the boundary between sequence-dependent and sequence-independent recognition in the middle of the −10 region coincides with the boundaries of strand opening [e.g., (*2*)] and of specific recognition by fragments of sigma factor (*22*).

Very similar patterns are found for K_d and k_d/k_a as a function of oligo sequence (compare Figure 4a and Figure 4b). Agreement between K_d and k_d/k_a is quantitative for the four oligos which bind most tightly, but for the other oligos the values of the two parameters differ considerably (up to a factor of 10 for ACGTGC) as is immediately apparent from the scales of the *y*-axes in Figure 4a,b. It is not clear whether this discrepancy, also seen in other experiments (see Table 1), is due to experimental artifact, or to an unrecognized fundamental feature of the reaction mechanism. In all cases, however, the trends displayed by K_d and k_d/k_a are qualitatively similar. We will report here values for k_a and k_d as determined by using eq 2, and K_d (or K_a) values as determined with eq 3. In the following sections we compare

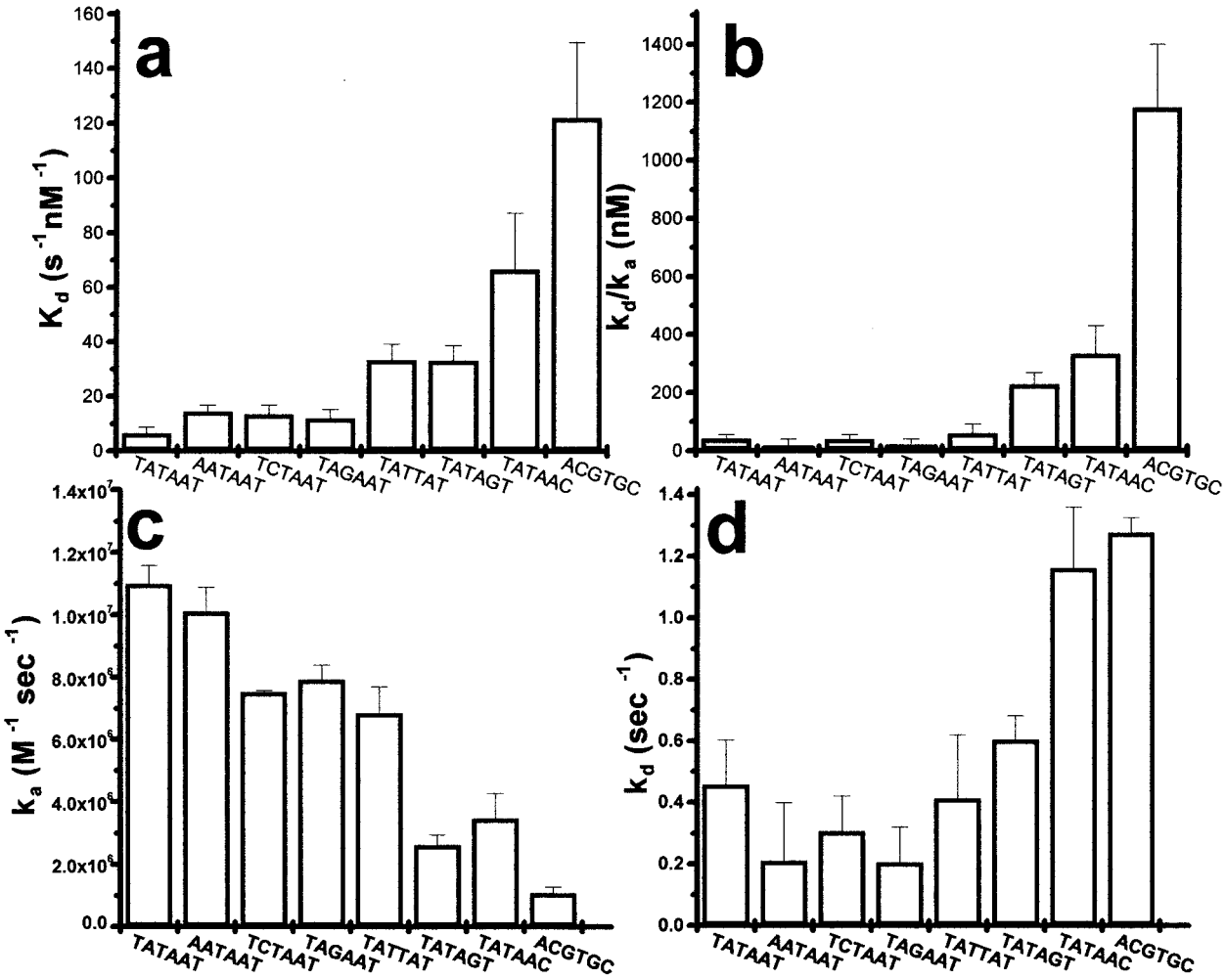

FIGURE 4: Sequence effects on the interaction of RNAP with oligos. Values for K_d, k_d/k_a, k_a, and k_d (determined at 25 °C) are shown in panels a, b, c, and d, respectively. Columns are labeled by −10 sequences of the oligos (see Figure 1).

the behavior of an oligo with a consensus −10 sequence to that of an oligo bearing a T-7C substitution.

In Figure 5 we show the dependence of K_a, k_a, and k_d on salt concentration. The slopes of plots of the logarithms of these respective parameters versus the logarithm of the salt concentration (*23*) indicate the number of ions released upon complex formation, in steps up to and including the processes limiting the association rate of the complex, and the number of ions taken up in dissociation. The salt dependencies are small, with the only clear effect that of KCl on k_a. The slope of the log−log plot is -2.0 ± 0.3, which would indicate the release of 2 ions in complex formation. The apparent discrepancy between this result and the fact that no significant effect is observed on the equilibrium constant can be ascribed to experimental error. To determine if the effects of KCl are due to the release of cations from DNA, and thus indicate ionic interactions between RNAP and the DNA, experiments were also conducted in solution with F^- as the anion. As F^- binds much less avidly to proteins than Cl^- [e.g., (*24*)], in such solutions, ion release from the protein can be ignored. Then salt effects can be ascribed uniquely to the release of cations from DNA as a result of neutralization of specific phosphates by positively charged groups on the DNA binding protein. As NaF was not found to have a significant effect, we conclude that the interaction of oligos with RNA polymerase is not accompanied by the release of cations and thus not driven by electrostatic interactions. The effects observed due to variation of [KCl] can then be interpreted as being due to the release of at most two Cl^- from RNAP upon complex formation (in general, Na^+ behaves identically to K^+ in these types of experiments).

In Figure 6a−c we show the dependencies of ln K_a, ln k_a, and ln k_d on temperature, as obtained in one representative experiment. The reason for using this representation instead of the more common Arrhenius plots (ln k vs $1/T$; $k = k_a$ or k_d) and van't Hoff plots (ln K_{eq} vs $1/T$; $K_{eq} = K_a$ or k_a/k_d) is that the latter plots displayed nonlinear behavior (not shown). The behavior of ln K_a observed here [strikingly similar to that of several other protein−nucleic acid interactions [e.g., (*25*)] has generally been interpreted as indicative of burial of hydrophobic groups upon complex formation, with concomitant release of bound water molecules (*26*). The "signature" of the hydrophobic effect is a large and negative change in the heat capacity, ΔC°_p, which is the temperature dependence of the enthalpy of the reaction: $\Delta C^\circ_p = d\Delta H^\circ_{obs}/dT$. The curve for the consensus oligo in Figure 6a is a fit to the data assuming the ΔC°_p is independent of temperature, when the following equation describes the temperature dependence of the equilibrium binding constant [e.g., (*25*)]:

$$\ln K_{eq} = (\Delta C^\circ_p/R)[(T_H/T) - \ln (T_S/T) - 1] \qquad (5)$$

where T_H and T_S are the temperatures at which, respectively,

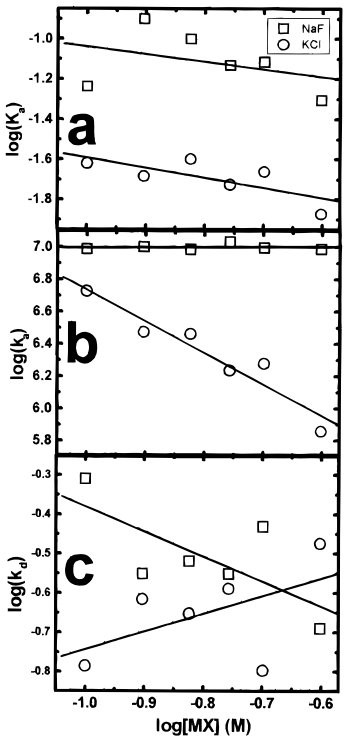

FIGURE 5: Salt dependencies of the interaction of RNAP with oligos. Data (obtained at 25 °C) are shown for the effects of KCl and NaF for the interaction of RNAP with the consensus oligo, as well as that bearing the C-7T substitution; log−log plots. (a) K_a; (b) k_a; (c) k_d. For these experiments, the 10 mM $MgCl_2$, normally present in our buffer, was omitted to allow the results to be more readily interpreted. The lines shown were obtained by linear regression.

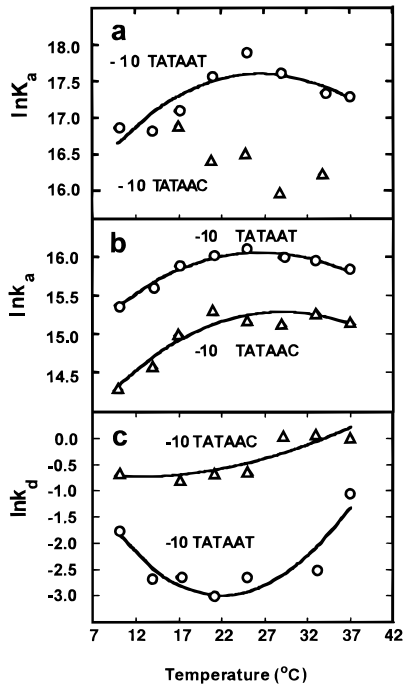

FIGURE 6: Temperature dependence of the interaction of RNAP with oligos. In panels a−c, ln K_a, ln k_a, and ln k_d are plotted as a function of temperature for the interaction of RNAP with both the consensus oligo (○) and that bearing the C-7T substitution (△). The data in panels a−c were fit to eqs 5, 8a, and 8b, respectively. The curves shown are based on these fits.

$\Delta H°_{obs}$ and $\Delta S°_{obs}$ are = 0. The data for K_a and k_a/k_d were fit to the three parameters $\Delta C°_p$, T_H, and T_S; average values for $\Delta C°_p$, as obtained from several experiments analogous to that shown in Figure 6, are shown in Table 2. The fits of k_a/k_d appear to be indicative of a less negative value of $\Delta C°_p$ for the interaction of RNAP with the T-7C oligo than with the consensus oligo. However in view of the large uncertainties in the values, it cannot be concluded that they are significantly different. The large negative values of $\Delta C°_p$ for both oligos are quite similar to that estimated for the interaction of RNAP with the P_R promoter [about 1 kcal M^{-1} K^{-1} (*25*)]. The temperature dependence of the rate of open complex formation at the P_R promoter also results in a nonlinear Arrhenius plot (*27*), which has been interpreted as reflecting a conformational change in the RNAP involving additional folding of the protein upon DNA binding (*26*). Thus, it is likely that, upon binding to an oligo, the RNAP undergoes a similar conformational change as it does upon interacting with promoter DNA.

Table 2: Heat Capacity Changes in RNAP−Oligo Interactions

		$\Delta C°_p$ (kcal M^{-1} K^{-1})		
oligo	K_a	k_a/k_d	k_a	k_d
−10 TATAAT	-0.9 ± 0.3^a	-2.3 ± 1^b	-0.9 ± 0.1^b	1.5 ± 1^b
−10 TATAAC	-0.8 ± 0.6^c	-1.2 ± 0.8^c	-0.9 ± 0.1^a	0.75 ± 0.3^a

[a] Average ± spread for 2 determinations. [b] Average ± SD for 3 independent determinations. [c] Meaningful fit only for 1 out of 2 determinations; standard errors based on computer fits of the data.

The values for the two rate constants k_a and k_d show extrema (see Figure 6b,c) which would not be expected if they were elementary rate constants. This behavior is indicative of a rapid equilibrium preceding the rate-limiting step in both the forward and reverse directions. Thus, even if the same step were rate-limiting in both directions, intermediates both preceding and following the rate-determining unimolecular step have to be invoked to explain the observation of extrema in both k_a and k_d. This is shown in eq 6:

$$\text{RNAP} + \text{oligo} \overset{K_1}{\rightleftharpoons} \text{RNAP}\cdot\text{oligo}_s \underset{k_b}{\overset{k_f}{\rightleftharpoons}} \text{RNAP}'\cdot\text{oligo}_s \overset{K_2}{\rightleftharpoons} \text{RNAP}'\cdot\text{oligo}_u \quad (6)$$

K_1 and K_2 are the equilibrium constants for the two rapid equilibrium steps, while k_f and k_b are the rate constants for the rate-limiting step in the forward and reverse directions, respectively. These need not be elementary rate constants, and their temperature dependence could include a $\Delta C°_p$ term. RNAP is the prevalent conformation of RNAP free in solution, RNAP′ the conformation of RNAP in the most stable complex with the oligo, oligo_s the oligo with the bases stacked, and oligo_u the oligo with unstacked bases. RNAP·oligo_s is the initial or "collision" complex between RNAP and an oligo, and RNAP′·oligo_u is the complex responsible for the observed increase in fluorescence. This equation is further considered in the Discussion. If the two rapid equilibria favor the beginning and end products shown in the equation, respectively, the expressions for the forward and reverse rate constants would be

$$k_a \approx K_1 k_f = K_1 K_a^{\#} k_B T/h \quad (7a)$$

$$k_d \approx K_2^{-1} k_b = K_2^{-1} K_b^{\#} k_B T/h \quad (7b)$$

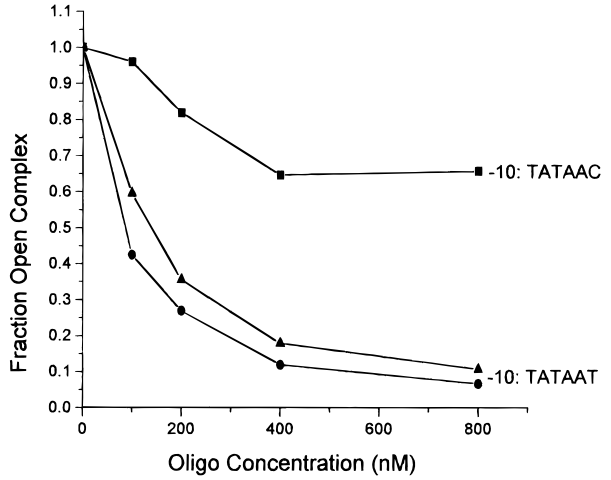

FIGURE 7: Oligos bearing the consensus −10 sequence compete with promoter DNA for RNAP binding. Reaction mixtures (37 °C) contained 2 nM radiolabeled promoter DNA, unlabeled oligo at the indicated concentration, and RNAP (50 nM). Promoter binding was monitored by gel mobility shift, and normalized to the extent of retention in the absence of oligo. Values shown are averages of two determinations. All oligos contained 2-AP, but not at the same positions. (■) T-7C; (●) consensus, both with 2-AP at −14 and −15; (▲) consensus, 2-AP at +1 and +3.

Here $K_a^{\#}$ and $K_b^{\#}$ are the equilibrium constants describing the position of the transition state with respect to the beginning and final components, respectively; k_B, Boltzmann's constant; and h, Planck's constant. Thus, the temperature dependence of the rate constants k_a and k_d would be a composite of the contributions from the pathway up to and including the transition state. The data in Figure 6b,c were fit to the following equations:

$$\ln k_a = \ln (k_B T)/h + (\Delta C^\circ_{p,a}/R)[(T_{H,a}/T) - \ln (T_{S,a}/T) - 1] \quad (8a)$$

$$\ln k_b = \ln (k_B T)/h + (\Delta C^\circ_{p,b}/R)[(T_{H,b}/T) - \ln (T_{S,b}/T) - 1] \quad (8b)$$

where $\Delta C^\circ_{p,a}$ and $\Delta C^\circ_{p,d}$ are the changes in heat capacity, up to and including the transition state, starting from either end of the reaction eq 6. Other symbols are as in ref *5*, but now applied toward the temperature dependence of the association and dissociation rate constants. The ΔC°_p values obtained with the use of eqs 5, 8a, and 8b (collected in Table 2) are of the order of ±1 kcal M^{-1} K^{-1}.

Sequence-specific recognition of the −10 promoter element is carried out by region 2.4 of sigma factor (*1*); the same region of sigma factor has been implied in the recognition of the −10 sequence on nontemplate oligos (*7*, *13*). Thus, promoter DNA and oligo are expected to compete for this region of RNAP, and not to be able to concurrently bind to the same RNAP. We tested this prediction by determining the effects of increasing amounts of unlabeled oligo on the interaction of radiolabeled promoter DNA with RNAP. As shown in Figure 7, competition of nontemplate strand oligos with formation of RNAP−promoter complexes is observed with oligos bearing the TATAAT sequence, but less so with oligos containing the C-7T substitution. This substitution in promoter DNA is known to dramatically reduce promoter strength. From the fact that oligo and promoter DNA compete for binding to RNAP, we conclude that indeed the oligo and promoter DNA bind to overlapping sites on RNAP.

DISCUSSION

We have characterized the kinetics and thermodynamics of sequence-dependent recognition by RNAP of a single-stranded nontemplate oligo. We propose that this interaction, by circumventing the process of strand separation, is a useful model system for studying particular aspects of RNAP−promoter interactions, such as the conformational change in RNAP. This contention is bolstered by the observed competition between oligo and promoter DNA (see Figure 7), as well as by the good agreement between the results obtained here with those obtained by others on the interaction of RNAP not only with oligos but also with promoters. Quite likely (*3*−*5*, *7*), the aromatic groups in sigma factor region 2.3, positioned on helix 14 in the crystal structure, interact with single-stranded promoter DNA in the establishment and/or maintenance of the open complex. The results presented here would be consistent with this assignment: the large negative ΔC°_p we observed could be due both to such hydrophobic interactions and to the conformational change in RNAP we invoke here (see below). On the other hand, we find little evidence for electrostatic interactions contributing favorably to the binding of oligos to RNAP. By ethylnitrosourea probing, Gilbert's group (*2*) identified 6 phosphates in the 22 base pair stretch of promoter DNA spanning the length of the oligo used here, as being important for open complex formation. In addition, pronounced effects of salt on the nonspecific binding of RNAP holoenzyme to single-stranded DNA were observed (*28*). As yet we do not understand the reasons for these discrepancies.

Our results on the kinetics of oligo−RNAP interaction are not compatible with a simple, one-step mechanism for the reaction. We summarize here the observations that lead to this conclusion. (1) The kinetic traces suggest that there may be an additional step, faster than that studied here (see Figure 2). (2) The association rate constants are affected, albeit not to a major extent, by the sequences of the oligos (Figure 4). Apparently, in the transition state some specific contacts between RNAP and the oligo are already established. This is not compatible with a simple, diffusion-limited binding reaction. (3) The association rate constant for the binding of oligos to RNAP is smaller by about an order of magnitude than that for forming an RNAP−promoter open complex: 7×10^6 M^{-1} s^{-1} for the consensus oligo (see Table 1) versus at least 10^8 M^{-1} s^{-1} for a consensus promoter under the same conditions (de Haseth et al., unpublished). Thus, a process other than formation of an initial collision complex of RNAP and oligo must be limiting. (4) The anomalous temperature dependencies of both the forward and dissociation reactions (Figure 6) require a more complex kinetic equation.

Based on the above observations, the general reaction eq 6 was proposed, which in each direction involves a rapid equilibrium prior to the rate-limiting step. We envisage that both RNAP and the oligo have to undergo conformational transitions from their predominant forms in solution. A conformational change in the RNAP (RNAP to RNAP′) is likely in view of the large negative ΔC°_p that accompanies complex formation. This step, the RNAP·oligo$_s$ to RNAP′·

oligo$_s$ conversion, would be rate-limiting. Based on eq 6, it is expected that k_{obs} would saturate at a high [oligo]. The fact that saturation is not observed could be due to weak binding of the oligo to RNAP in the predominant conformation in solution: if even the highest [oligo] used still is $\ll 1/K_1$, then no curvature is observed in the k_{obs} versus [oligo] plot. This is analogous to a two-step reaction, corresponding to the first two steps in ref *6*, discussed by Johnson (*29*).

With the consensus oligo and that bearing the T-7C substitution, similar $\Delta C°_p$ values are obtained within experimental error (see Table 2). It therefore seems likely that these two oligos require a similar conformational change in RNAP in order to form the complex we have monitored in these studies. It is possible to interpret observed values of $\Delta C°_p$ in terms of the surface area of buried nonpolar groups. Record and co-workers (*25*) proposed the empirical relationship $\Delta C°_p/\Delta A_{np} = -0.3$ cal K^{-1} Å^{-2}, with ΔA_{np} the surface area (in Å^2) that gets buried. For a $\Delta C°_p$ of 1 kcal M^{-1} K^{-1} or greater, as found here for the interaction of RNAP with a single-stranded oligo, 3000 Å^2 or more of nonpolar surface could be buried upon the binding of the consensus oligo. This is much more than the surface area on the protein which can be covered directly by the oligo. Based on the surface areas of the bases, the oligo would have at most about 250 Å^2 of nonpolar surface. The region of sigma factor interacting with the nontemplate strand of promoter DNA is likely nonpolar, so by direct interaction maximally about 500 Å^2 could be buried, which is only 16% of the total required by Record's estimation. The rest of the buried surface would be due to the folding of regions of RNA polymerase which would accompany a major conformational change of the enzyme. This might involve the closing of the "jaws" of the polymerase which are thought to form a sliding clamp which keeps the enzyme associated with DNA during the elongation process (*15*, *16*, *30*).

The interpretation of the nonlinear Arrhenius plots we observed in terms of a model involving a linear dependence on temperature of the $\Delta H°_{obs}$ for the binding reaction may not be the only one consistent with such behavior. Lohman and co-workers (*31*) have shown that similar effects could also be obtained for processes involving coupled equilibria, where one of the two equilibria would have a positive, but temperature-independent $\Delta H°_{obs}$. In our case this possibly could be the unstacking of the bases on the oligo.

The similarity in the values for the $\Delta C°_p$ of the interactions of RNAP with oligos and with promoters suggests that similar conformational changes of RNAP could be involved in both processes. This underscores the value of the interaction with oligos as a model system for studying facets of the process of open complex formation at promoters. At the same time, the rate constant for the interaction of RNAP with promoters is an order of magnitude greater than that for the interaction with oligos. Additional favorable interactions between the promoter and RNAP would have to stabilize the transition state for the conformational change by only 1.2 kcal/mol in order to accomplish this. The −35 region of the promoter could be responsible for this stabilization. However, we cannot exclude an alternative possibility, namely, that promoter DNA dissociates more slowly from an initial (collision) complex than an oligo, again due to interactions with the −35 region of the promoter. In this case, the differences in the observed rates would be due to the relative population of the initial complex, rather than to the relative rates with which the promoter DNA and the oligo would induce conformational changes in RNAP.

ACKNOWLEDGMENT

We thank Michael Strainic, Jr., for determining the activities of the RNAP preparations used in this work and M. Zupancic and Drs. Tim Lohman and Tom Record, Jr., for helpful discussions.

REFERENCES

1. Lonetto, M., Gribskov, M., and Gross, C. A. (1992) *J. Bacteriol. 174*, 3843−3849.
2. Siebenlist, U., Simpson, R. B., and Gilbert, W. (1980) *Cell 20*, 269−281.
3. Aiyar, S. E., Juang, Y.-L., Helmann, J. D., and deHaseth, P. L. (1994) *Biochemistry 33*, 11501−11507.
4. Juang, Y.-L., and Helmann, J. D. (1994) *J. Mol. Biol. 235*, 1470−1488.
5. deHaseth, P. L., and Helmann, J. D. (1995) *Mol. Microbiol. 16*, 817−824.
6. Chen, Y.-F., and Helmann, J. D. (1997) *J. Mol. Biol. 267*, 47−59.
7. Huang, X., Lopez de Saro, F. J., and Helmann, J. D. (1997) *Nucleic Acids Res. 25*, 2603−2609.
8. Roberts, C. W., and Roberts, J. W. (1996) *Cell 86*, 495−501.
9. Savinkova, L. K., Baranova, L. V., Knorre, V. L., and Salganik, R. I. (1988) *Mol. Biol. 22*, 651−656.
10. Savinkova, L. K., Sokolenko, A. A., Tulokhonov, I. I., Knorre, V. L., Salganik, R. I., Ven'yaminova, A. G., Repkova, M. N., and Komarova, N. I. (1993) *Mol. Biol. 27*, 33−37.
11. Savinkova, L. K., Sokolenko, A. A., Kel, A. V., Tulokhonov, I. I., Kumarev, V. P., Baranova, L. V., Rar, V. A., and Salganik, R. I. (1996) *Mol. Biol. 30*, 188−191.
12. Severinova, E., Severinov, K., Fenyo, D., Marr, M., Brody, E., Roberts, J. W., Chait, B. T., and Darst, S. A. (1996) *J. Mol. Biol. 263*, 637−647.
13. Marr, M. T., and Roberts, J. W. (1997) *Science 276*, 1258−1260.
14. Callaci, S., and Heyduk, T. (1998) *Biochemistry 37*, 3312−3320.
15. Record, M. T., Jr., Reznikoff, W. S., Craig, M. L., McQuade, K. L., and Schlax, P. J. (1996) *Escherichia coli and Salmonella, cellular and molecular biology* (Neidhardt, F. C., Ed.) pp 792−820, ASM Press, Washington, DC.
16. deHaseth, P. L., Zupancic, M., and Record, M. T., Jr. (1998) *J. Bacteriol. 180*, 3019−3025.
17. Burgess, R. R., and Jendrisak, J. J. (1975) *Biochemistry 14*, 4634−4638.
18. Gonzales, N., Wiggs, J., and Chamberlin, M. J. (1977) *Arch. Biochem. Biophys. 182*, 404−408.
19. Sullivan, J. J., Bjornson, K. P., Sowers, L. C., and deHaseth, P. L. (1997) *Biochemistry 36*, 8005−8012.
20. Barne, K. A., Bown, J. A., Busby, S. J. W., and Minchin, S. D. (1997) *EMBO J. 16*, 4034−4040.
21. Moyle, H., Waldburger, C., and Susskind, M. M. (1991) *J. Bacteriol. 173*, 1944−1950.
22. Dombroski, A. J. (1997) *J. Biol. Chem. 272*, 3487−3494.
23. Record, M. T., Jr., Lohman, M. T., and de Haseth, P. (1976) *J. Mol. Biol. 107*, 145−158.
24. Lohman, T. M., and Ferrari, M. E. (1994) *Annu. Rev. Biochem. 63*, 527−570.
25. Record, M. T., Jr., Ha, J. H., and Fisher, M. A. (1991) *Methods Enzymol. 208*, 291−343.
26. Spolar, R. S., and Record, M. T., Jr. (1994) *Science 263*, 777−784.
27. Roe, J. H., Burgess, R. R., and Record, M. T., Jr. (1985) *J. Mol. Biol. 184*, 441−453.

28. deHaseth, P. L., Lohman, T. M., Burgess, R. R., and Record, M. T., Jr. (1978) *Biochemistry 17*, 1612−1622.
29. Johnson, K. A. (1992) *Enzymes (3rd Ed.) 20*, 1−61.
30. Schickor, P., Metzger, W., Werel, W., Lederer, H., and Heumann, H. (1990) *EMBO J. 9*, 2215−2220.
31. Ferrari, M. E., and Lohman, T. M. (1994) *Biochemistry 33*, 12896−12910.

BI980980O